Determination of the Electron to Pion response ratio of the NuTeV detector

David A. Moscol, Georgia Intitute of Technology Donna Naples, Kansas State U

August 28, 1998

Abstract

The following paper focuses on the results of a calibration study carried out from June 15 through August 28 1998 at Fermilab's NuTeV experiment. The study consisted of measuring two calibration markers, C_e and $C_\pi$over different calibration periods to observe the consistency in their values. This paper presents the results of measurements of the electron to pion response ratio as a function of energy for the NuTeV (E815) detector at medium to highenergy tunes. The analysis consists of generating electron response and pion response values from multiple testbeam runs and comparing them to that of previous calibrations to assess the difference between the C_e/C_π ratios.

1 Introduction

The NuTeV neutrino detector relies on a particle beam originating from the Tevatron for its operations. The actual neutrino beam is the result of an accelerated proton beam. First, hydrogen ions are produced through the insertion of a cesium cathode in hydrogen gas. The ions then proceed to the Cockroft-Walton, an electrostatic device which accelerates the particles by passing them through a series of electrostatically generated potential drops, increasing their energy to 750 GeV. The ions then travel through the LINAC, Fermilab's linear accelerator, which accelerates the particles to 200 MeV by employing a series of radio frequency cavities. Following the LINAC, the ions are put through a carbon foil which serves to strip electrons away, leaving a proton beam. The protons then enter the Booster, a synchrotron 140 meters in diameter. The synchrotron, a circular device which uses a magnetic field to keep protons at a particular orbit and accelerates them using an electric field along the ring, increases the protons' energy to 8 GeV. The Booster injects the proton beam into the Main Ring which is also a synchrotron (2 kilometers in diameter). The Main Ring uses 1000 magnets to direct the proton beam, accelerating them to 150 GeV. The acceleration process is completed at the Tevatron, a superconducting synchrotron operating at 40 kiloGauss. The Tevatron's superconducting magnets accelerate the proton beam to 800 GeV. While on fixed-target runs, the Tevatron operates on a 60 second cycle. Each cycle fills the ring with approximately 10^{13} protons. The protons remain at their maximum energy (800 GeV) for about one third of the cycle (20 seconds). They are removed form the Tevatron in fast and slow "spills." The fast spills last one millisecond while the slow spills last two seconds. Only protons from the fast spills are used for the neutrino beam. The protons exiting in the fast spill are collided with a 33 centimeter Beryllium-Oxide target and a meson beam emerges from this interaction. After being focused by three quadropole magnets in the beamline, the mesons pass through a 320 meter decay zone. Here, about one tenth of the pions and kaons decay in flight, yielding mostly muons and muon neutrinos. The rest of the beam is directed into a 6 meter aluminum block followed by steel shielding. The NuTev detector is located 915 meters past the shielding. Therefore, neutrinos and muons entering the aluminum beam dump come across 241 meters of steel shielding and 582 meters of earth berm. This is enough material to absorb the muons in the beam, allowing only neutrinos to reach the detector. Nevertheless,

some neutrinos interact with the earth within the berm, generating a source of muons that does make it to the detector. This "interference" is corrected in the process of analyzing the data from the detector. The calibration process relies on the use of two testbeams: one composed mostly of electrons and the other of pions. These two testbeams comprise the types of particles generated by neutrino interactions in the detector, which is why they are y used for calibration purposes. The impact of a neutrino on a nucleon in the detector results in the decomposition of the nucleon into hadrons, principally pions, kaons, protons and neutrons. These hadrons, in turn, interact and decay in what is known as a hadron shower, which spreads through the calorimeter until all its energy is absorbed. This means the hadron shower moves through the scintillation counters, drift chambers and steel plates of the detector. The total energy of the shower can be assessed by observing the fraction that is deposited in the counters. The amount of energy deposited by a high energy particle in a material is mostly independent of the particle type and how much energy it possesses. This deposited energy is referred to as minimum ionizing energy. When hadrons pass through the calorimeter, the interactions result in showers of secondary particles. In contrast to the minimum ionizing energy, these interactions do depend on energy. Consequently, the number of particles present in the secondary shower is directly proportional to the energy of the original particle. When each secondary particle passes through a counter, it deposits the same amount of energy, the minimum ionizing energy. Therefore, dividing the total energy measured in a single counter by the minimum ionizing energy yields the number of minimum ionizing particles (muons), or MiPs, that passed through that particular counter. These hadronic showers, normally spawned by neutrino events, can be reproduced for calibration purposes using the electron and pion testbeams. The electron response marker, C_e, represents the ratio of the energy deposited in the first twenty counters of the detector (esum20) to the mean test beam momentum (ptb). Esum20 is measured in mips and ptb in GeV/c2. Therefore, C_e is in fact the conversion factor between MiPs and GeV. The energy deposition in the first twenty counters corresponds to the hadronic shower energy resulting from the interaction of an electron in the detector. However, as described above, the electron test beam is inevitably contaminated with muons. Given their higher index of penetration, muons in the test beam may transcend the 20 counter mark depositing little energy. This results in a lower C_e value for the event in question. Likewise, the

pion response marker, C_π, also represents the ratio of the energy deposited in the first twenty counters of the detector (esum20) to the mean test beam momentum (ptb) and the conversion factor between MiPs and GeV, in this case for pion events. The hadronic shower is less energetic than that of the electron, therefore C_π is less than C_e, resulting in a ratio greater than one.

2 Apparatus

The NuTeV detector is composed of two sections: a 690 ton target calorimeter and a muon spectrometer. The calorimeter, which is the section used for calibration, is 17.7 meters in length and is comprised of six modules called carts. Each Cart, in turn, is made up of 28 steel plates, fourteen scintillation counters and seven drift chambers. The scintillation counters are installed between every two plates while the drift chambers are located between every four plates. Part of the energy measurement in the calorimeter is made by the scintillation counters, which are 10 x 10 feet x 1 inch tanks containing mineral oil and scintillating fluors. At each corner of the tank lies a photomultiplier tube which measures the energy deposited and amplifies the energy signal through a simple application of the photoelectric effect. Any charged particle, the direct product of an interaction in the detector, passes through a scintillation counter exciting the fluors in the oil, resulting in the emission of ultraviolet light. The UV light is absorbed by a second set of fluors which in turn emit visible blue light. The reason for the intentional wavelength shift is that blue light lasts longer in the oil and when emerging below the oil's critical angle, can be easily sent to the counter's edge through total internal reflection. Once at the edge of the counter, the wavelength is changed again, this time to green, in order to meet design specifications of the phototubes. Once the light gets to the phototubes, the detector's electronics interpret the signal accordingly. The calorimeter's drift chambers serve to track muons resulting from neutrino interactions. The drift chambers is able to record the presence of a charged particle by detecting the emission of ionization electrons. Each drift chamber is made up of 24 horizontal and 24 vertical cells, each of which measures 5 inches wide and 0.75 inches thick and contains three wires. The drift chambers contain a mix of argon and ethane in equal proportions. Due to its noble gas properties, argon can be easily ionized by a passing charged particle with enough energy. After such an event, the ions and electrons are separated by the applied electric field in the chamber. The electrons "drift" toward the cell wires, accelerating and producing a second set of ionizations. The ethane serves to quench the UV photons emitted in the argon as the electrons move toward the cell wires, thus controlling what would otherwise be an large amount of interfering charge in the chamber. The second component of the detector is the muon spectrometer. This spectrometer is comprised of three toroid-shaped magnets and 10 square foot

drift chambers arrays. Each magnet is called a cart and is separated into eight cylinders, 8 inches thick each, called washers. The muons are tracked by the 25 drift chambers in the spectrometer section, each of which contains one-wire cells.

3 Method

All events from a particular test beam run are archived on tape for analysis. The analysis process is carried out in three steps:

• The gzipped data file is run through the cruncher, which returns an ntuple file containing all the variables of interest for a particular test beam run

• The ntuple file is interpreted using a kumac routine, written by Donna Naples, which generates a gaussian curve showing the mean C_e or C_π value

• The C_e and C_π values for the respective energy tunes are juxtaposed with the previous values to assess any changes

The data cruncher uses the latest iteration of the calibration constants necessary to calculate the process variables. The kumac routine also subjects the test beam data to a series of filtering data cuts applied to the electron and hadron samples. One of these cuts is implemented to exclude the muon effects described above. Although the pion beam is also subject to muon interference, it is to a lesser degree. Thus, a different cut is applied to the pion beam to account for muons. The C_e and C_π values for any given energy tune are the arithmetic mean of the C_e and C_π values for the individual test beam runs of that energy. The beam data was also subjected to a temperature correction to account for the phototubes' sensitivity to temperature differentials. However, the accuracy of this correction came into question during the data analysis. Consequently, only a fraction of the results include this correction. The majority of the data presented in the tables below is not subject to a temperature correction.

4 Data

The series of tables below present the C_e and C_π data separately and then as a ratio for both values that are temperature corrected and those that are not.

Table 1: Electron Data with Temperature Correction

TB RUN	TUNE	P_{TB} (GeV)	$C_e \pm \Delta$
721	30	29.1	5.18±0.006
715	50	48.3	4.93±0.005
799	50	48.3	4.90±0.005
716	75	73.4	4.82±0.005
798	75	73.4	4.90±0.006
717	100	96.2	4.81±0.006
851	120	113.7	4.88±0.006
852	150	140.4	4.87±0.006
819	170	161.5	5.07±0.005
853	170	161.5	4.88±0.006

Table 2: Pion Data with Temperature Correction

TB RUN	TUNE	P_{TB} (GeV)	$C_\pi \pm \Delta$
96	30	29.1	4.59±0.004
653	30	29.1	4.52±0.008
688	30	29.1	4.67±0.007
89	50	48.3	4.66±0.006
87	75	73.4	4.67±0.004
420	75	73.4	4.64±0.005
598	75	73.4	4.61±0.002
720	100	96.2	4.61±0.004
752	100	96.2	4.47±0.005
98	120	113.7	4.67±0.004
173	120	113.7	4.63±0.004
662	120	113.7	4.65±0.004
1086	120	113.7	4.57±0.004
428	150	140.4	4.89±0.006
102	170	161.5	4.91±0.003
183	170	161.5	4.83±0.004
431	170	161.5	4.93±0.004
560	170	161.5	4.97±0.003
673	170	161.5	4.91±0.004

Table 3: Electron-Pion Ratio with Temperature Correction

TUNE	P_{TB} (GeV)	ratio±error
30	29.2	1.13± 0.003
50	48.5	1.06± 0.003
75	73.7	1.05± 0.000
100	96.7	1.06± 0.000
120	115.5	1.05± 0.000
150	142.5	1.00± 0.000
170	164.3	1.01± 0.000

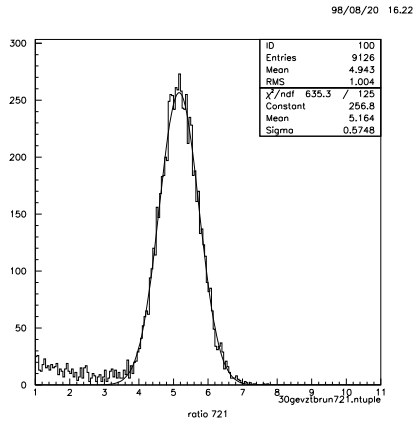

Figure 1: Electron Response Marker, C_e, for the 721 test beam run.

Figure 1 shows a gaussian distribution for a specific electron test beam run, in this case at 30 GeV. It is easy to observe the muon background in the plot, located on the lower left side of the curve.The beginning of the solid curve fit marks where the muon cut was placed. The vertical axis represents the number of events while the horizontal axis shows the C_e values. Similarly, Figure 2 depicts a distribution for a pion test beam run, also at 30 GeV. It can be seen that the muon background in the pion plot is considerably less than in the electron test beam plot. Both these plots are representative of the nature of the test beam distribution and so have been included as typical examples of the data group. However, there were several exceptional runs

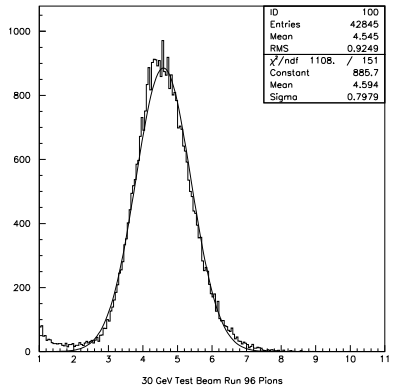

Figure 2: Pion Response Marker (C_π) for the 96 test beam run.

that did not follow the expected distribution. 30 GeV electron test beam runs 37 through 40 were thrown out of the data group because they contained too few events to represent an accurate value of C_e. These runs also present a high statistical error due to their low event count. Figure 3 shows the plot for test beam run 38. Also, 30 GeV electron runs 806, 807, 923, 927, and 50 GeV electron runs 800 and 805 constitute special runs and were thus excluded. Figure 4 shows the plots for these special runs. Runs 806, 927 and 805 were conducted with two additional 2" steel plates, separated by a counter, added to the first plate of the detector. Runs 807, 923 and 800 were conducted with two additional steel plates, one being 2" and the other 1", separated by a counter, also added to the first plate of the detector. As one would expect, those runs where both plates were 2" wide exhibited a lower C_e value than those with one 2" and one 1" plate. This is because the incoming electron interacts sooner in those runs where more additional steel is present.

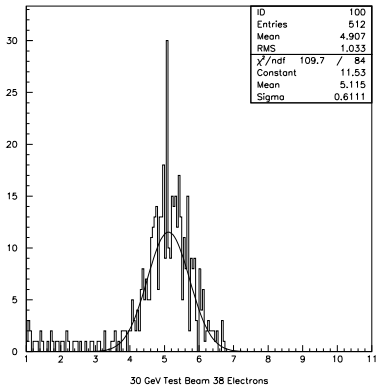

Figure 3: This Test Beam Run contained too few events.

5 Conclusion

The final result of this project is given by Figure 5. This graph shows the total C_e/C_π ratio for each of the energy tunes in question. There is no obvious pattern in the difference between the two calibration periods. However, the present ratio seems to increase over the old one as the energy tune becomes higher. At 30 GeV the old ratio was higher, at 50 GeV they are identical and by 75 GeV the new ratio is definitely higher than the old one. From this point on, the new C_e/C_π always lies above the old one. The question of immediate concern is what gives rise to this discrepancy. Firstly, the new values were obtained using a new iteration of the calibration constants that are used by the Fortran routine cruncher. Since these constants differ from the ones used for the previous calibration, the new C_e/C_π ratios will necessarily be different from the old ones. Therefore, the key fundamental difference lies in these constants, since no temperature correction was employed for the final results. Nevertheless, the fact that the two sets of C_e/C_π ratios do not vary wildly from one another indicates a good degree of consistency for the NuTeV detector. The largest C_e/C_π discrepancy (at 75 GeV) was less than 0.050, a very reasonable differential and easily accounted for by the change in calibration constants. It is also noteworthy that the new calibration did not affect all the energy tunes by the same magnitude. That is to say, each of the C_e/C_π varied by a different amount and the 50 GeV value did not change

at all. Given that an expected result was obtained from the new calibration, it is fair to assume that all the testbeam runs included in this analysis were good. Regardless, the appendix contains a list of bad testbeam runs.

6 Appendix

This appendix contains useful information that was not directly pertinent to the main discussion of C_e/C_π values. Within are included all the testbeam runs that were thrown out because of flaws.

Table 4: Electron Data without Temperature Correction

TB RUN	TUNE	P_{TB} (GeV)	$C_e \pm \Delta$
721	30	29.1	5.16±0.006
30	30	29.1	5.05±0.008
715	50	48.3	4.96±0.005
799	50	48.3	4.81±0.005
25	50	48.3	4.97±0.007
477	50	48.3	4.99±0.009
772	50	48.3	4.96±0.005
778	50	48.3	5.12±0.005
782	50	48.3	4.88±0.006
716	75	73.4	4.81±0.005
22	75	73.4	4.86±0.007
23	75	73.4	4.87±0.009
773	75	73.4	4.86±0.005
777	75	73.4	5.02±0.006
783	75	73.4	4.92±0.008
786	75	73.4	4.92±0.008
921	75	73.4	4.83±0.005
1074	75	73.4	5.96±0.006
1075	75	73.4	5.48±0.005
1076	75	73.4	5.01±0.005
1077	75	73.4	4.96±0.004
1078	75	73.4	4.72±0.006
717	100	96.2	4.79±0.006
12	100	96.2	4.89±0.008
13	100	96.2	4.88±0.007
774	100	96.2	4.82±0.006
776	100	96.2	4.98±0.007
784	100	96.2	4.95±0.007
785	100	96.2	4.95±0.007
797	100	96.2	4.92±0.006
922	100	96.2	4.86±0.006
851	120	113.7	4.88±0.006
856	120	113.7	5.04±0.006
817	120	113.7	4.85±0.007
852	150	140.4	4.88±0.006
818	150	140.4	5.09±0.005
831	150	140.4	5.13±0.006
855	150	140.4	5.01±0.006
858	150	140.4	4.96±0.008
819	170	161.5	5.07±0.005
853	170	161.5	4.89±0.006
854	170	161.5	5.02±0.005

Table 5: Pion Data without Temperature Correction

TB RUN	TUNE	P_{TB} (GeV)	$C_\pi \pm \Delta$
96	30	29.1	4.59±0.004
653	30	29.1	4.51±0.008
688	30	29.1	4.70±0.007
89	50	48.3	4.67±0.006
87	75	73.4	4.68±0.004
420	75	73.4	4.55±0.005
598	75	73.4	4.61±0.002
720	100	96.2	4.61±0.004
752	100	96.2	4.46±0.005
98	120	113.7	4.67±0.004
173	120	113.7	4.63±0.004
662	120	113.7	4.66±0.004
1086	120	113.7	4.56±0.004
428	150	140.4	4.89±0.006
102	170	161.5	4.91±0.003
183	170	161.5	4.83±0.004
431	170	161.5	4.93±0.004
560	170	161.5	4.98±0.003
673	170	161.5	4.92±0.004

Table 6: Electron-Pion Ratio without Temperature Correction

TUNE	P_{TB} (GeV)	ratio±error
30	29.1	1.11±
50	48.3	1.06±
75	73.4	1.09±
100	96.2	1.08±
120	113.7	1.06±
150	140.4	1.02±
170	161.5	1.02±

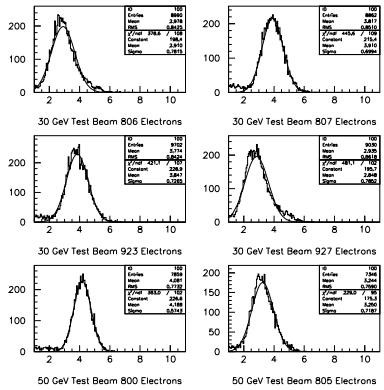

Figure 4: These Test Beam Runs look unconventional because they were used for a different purpose.

Table 7: Flawed Test Beam Runs

TB RUN	TUNE	Flaw Description	
37	30	Too few events	
38	30	Too few events	
39	30	Too few events	
40	30	Too few events	
980	75	Too few events	
979	75	Too few events	
775	100	Too few events	
968	120	Too few events	
969	120	Too few events	
814	120	Too few events	
813	120	Too few events	
816	120	Too few events	
967	150	Too few events	
970	150	Too few events	
827	170	Too few events	
832	170	Too few events	

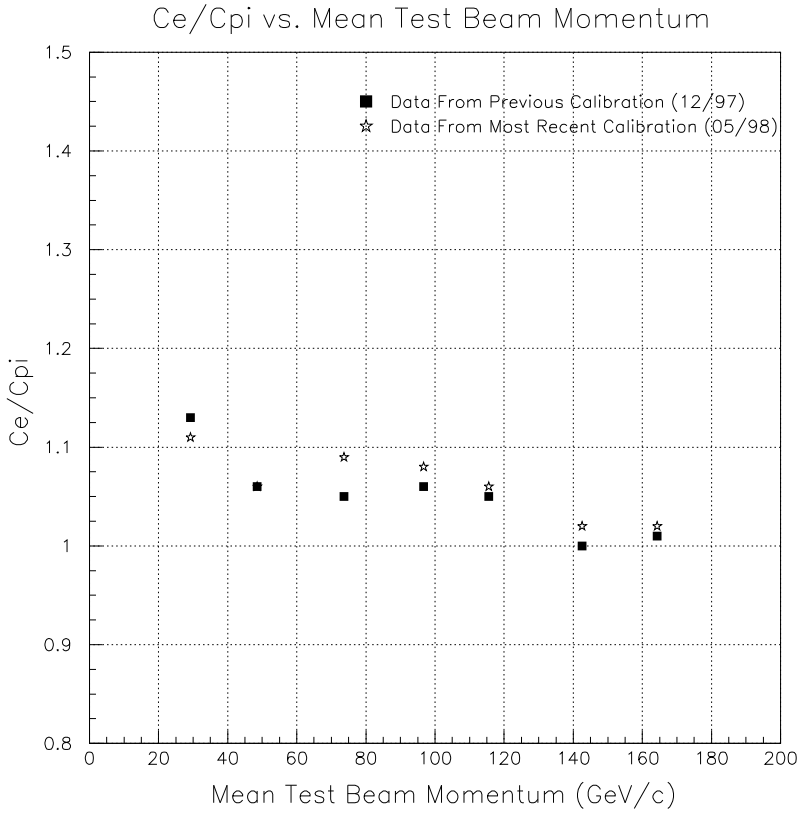

Figure 5: Final C_e/C_π ratios as a function of testbeam momentum.